A Dual Band Monopole Antenna with Slots for Wireless Applications

Mohaimen Q. Algburi
College of Communications Engineering, University of Technology- Iraq, Baghdad, Iraq
mohaimen.q.khalaf@uotechnology.edu.iq

Mustafa Ghanim
College of Communications Engineering, University of Technology- Iraq, Baghdad, Iraq
mustafa.g.rzooki@uotechnology.edu.iq (corresponding author)

Ayman N. Muhi
College of Communications Engineering, University of Technology- Iraq, Baghdad, Iraq
aymen.n.muhi@uotechnology.edu.iq

Received: 29 March 2025 | Revised: 26 April 2025 and 10 May 2025 | Accepted: 15 May 2025

 DOI: https://doi.org/10.48084/etasr.11209

ABSTRACT

A compact dual-band portable antenna operating at 1.8 and 2.4 GHz was designed and implemented for various applications of communication systems, such as wearable and wireless device systems. The dual-band operation of the proposed antenna enables it to be used in a rapidly changing array of applications that meet the demands of modern communication technologies, such as the Global System for Mobiles (GSM) at 1.8 GHz, Digital Communication System (DCS) at 1.71–1.88 GHz, Industrial, Scientific, and Medical (ISM) band at 2.4 GHz, Wi-Fi at 2.4–2.454 GHz, and Bluetooth at 2.4–2.5 GHz. The design is also based on slot technology for miniaturization, achieving dual-band operation, and reducing the unwanted surface currents. The proposed method miniaturizes the antenna while achieving good efficiency in both frequency bands. The preliminary design of the antenna was performed by simulation using the Computer Simulation Technology (CST) Studio Suite, the most advanced electromagnetic simulator. The results indicate excellent radiation efficiency of 92.59% and 96.75% at 1.8 and 2.45 GHz, respectively, as well as gain, $S_{11} \leq -10$ dB, and radiation pattern stability. Consequently, the compact size and high performance of the proposed antenna offers excellent opportunities for wearable or portable devices and other wireless communication systems.

Keywords-wireless applications; monopole antenna; slot antenna; FR4; global system for mobiles

I. INTRODUCTION

In wireless communication systems, there are numerous applications of multi-band and dual-band antennas that play a vital role in facilitating efficient wireless communication between different devices [1]. These antennas operate in different frequency ranges and are designed to ensure seamless connectivity and enhance the overall wireless communication experience [2-4]. Among the various types of antennas, patch antennas remain the most commonly used in wireless applications [5, 6]. This is primarily due to their small size, cost-effectiveness, ease of fabrication, and compatibility with integrated circuits [7]. However, these devices have limitations, including singularity of resonance frequency, polarization impurity, enhanced physical dimensions, limited gains, low efficiency, and narrow impedance bandwidth [8, 9]. However, slot antennas are desirable, particularly in the case of planar antenna structures, for their multi-operating band antenna uses [10]. Moreover, such an antenna is an important element for microwave systems, due to its inherent characteristics in terms of wider bandwidths and covering less space [11, 12]. Modern antenna designs have emerged to satisfy specific application needs, including in-body, on-body, and sensor-based systems, and other requirements [13-15]. The first requirement for achieving these targets requires a full comprehension of the existing literature, which provides the necessary knowledge before developing further [16, 17].

Modern communication systems demand multiband antennas with desirable impedance matching and highly directive shapes across various frequency bands [18, 19]. However, antenna optimization has always been a subject of interest for researchers in wireless communication systems [20, 21]. At every stage of optimizing an antenna, problems are encountered in obtaining performance in terms of gain, bandwidth, return loss, size reduction, and many other parameters as per the operational frequency of the antenna. In addition, a reduction in the size of the antenna often leads to a reduction in its efficiency and gain [22]. Therefore, achieving smooth dual-band functionality while maintaining the desired radiation patterns is challenging. Moreover, antennas must overcome any neighboring networks that emit electromagnetic interference. They should also be designed to tolerate different operating circumstances and maintain durability and flexibility. These issues must be solved with advanced antenna designs and selective materials to enable a dependable communication in the crowded and diverse wireless environment [23].

The demand for dual or multiband features has risen significantly due to their use in wireless local area networks including Bluetooth, WLAN, and WiMAX and ISM applications. Modern communication standards require a single-antenna system that can handle all frequency bands because it provides coverage across multiple bands while minimizing the system size. Planar slot antennas have emerged as suitable systems for achieving broadband or multiband operations, enabling multiple standard service coverage. They also constitute potential solutions for achieving broadband and multiband operations for multi-standard services. Various techniques have been introduced to improve the microstrip slot antenna parameters for realizing multiband functionality. These include the use of metamaterials [24], parasitic elements [25], Defected Ground Structures (DGS) [26], and innovative feeding techniques [27].

This study introduces a strategy for incorporating small rectangular slots into an antenna construction to achieve a high-gain dual-band radiating antenna. The antenna structure comprised a monopole with rectangular slots and a single wing. The small rectangular slots on the radiator adjunct are symmetrically arranged to provide dual-band functionality. The position of the monopole is carefully adjusted to achieve a resonant frequency of 1.8 GHz, and with the use of slot techniques, the dual-band is achieved. The antenna performance was analyzed using the CST Studio Suite, electromagnetic wave simulator. The antenna realized a return loss <-10 dB with stable radiating patterns and high gain at the desired frequency ranges of 1.8 and 2.4 GHz for wireless devices and ISM applications.

II. RECTANGULAR SLOT ELEMENT

The geometrical representation of the proposed slotted square patch antenna is shown in Figure 1. The proposed antenna comprised a copper square patch with dimensions of 20 mm × 20 mm. The square area in the antenna design contains 4 slots of the same length (*Ls* = 5 mm) and width (*Ws* = 1.65 mm) based on the X and Y axes and 8 slots of the same length and width are cut off the edge of the square area.

As depicted in Figure 1, the slots in the vertical (Y axis) direction cut the current running the same parameter to the X axis. Therefore, the TM100 mode is longer and has a lower resonance frequency. Similarly, the horizontal slots slice the current flowing along the Y-axis. The TM010 mode is longer and has a lower resonance frequency. For etched slots into the patch structure, the TM100 and TM010 are both influenced simultaneously and in the same way. This means that they have the same resonance frequency. As the dimensions of the slots *Ls* increase, the resonance frequencies decrease. Depending on the feeding mechanism, both types can be activated simultaneously or separately. As the length of the slots *Ls* increases, the resonance frequency (high frequency) drops faster. This is because the vertical and horizontal slots cut off the current of the TM110 mode. The modes resulting from the slots can be considered as deformed versions of those mentioned above.

The slot technique is selected for this study because it is simple, easy to fabricate and operates well with the conventional Printed Circuit Board (PCB) technologies. Using the slot technique, complex fabrication processes or expensive production methods are avoided since it enables an easy modification of the ground plane or radiator to achieve dual resonances through current distribution manipulation.

To study how the slot length *Ls* affects the resonant frequencies of TM100, TM010, and TM110, a 20 mm wide patch was used on a low-cost FR-4 substrate with a loss tangent of 0.025, a thickness of h = 1.6 mm, and a relative transmittance ε_r = 4.3. Figure 2 illustrates the influence of changing the slot length on the antenna performance. It is worth noting that the design, analysis, and simulation were performed using the CST 2019 software. As the slot length *Ls* increases, the resonant frequencies (high frequency) decrease because they are affected by the horizontal and vertical slots.

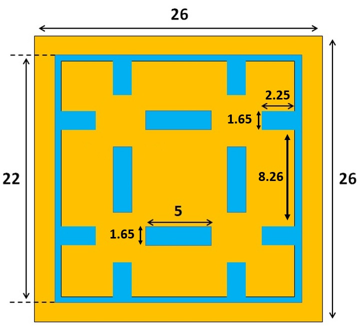

Fig. 1. The proposed design of the square patch with slots. All dimensions are in mm.

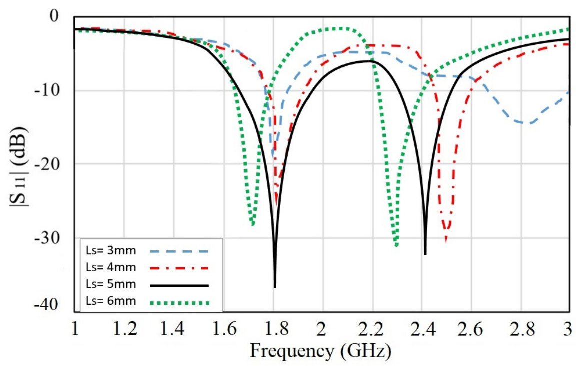

Fig. 2. Impact of varying slot lengths *Ls* on antenna performance.

III. PROPOSED ANTENNA DESIGN

Figure 3 portrays the geometric configuration of the proposed antenna. The proposed design consists of a conventional monopole and a single wing with a square radiating element and a ground plane on the other side. The proposed antenna was developed to achieve two frequency bands that matched the required design. The square slot monopole antenna operates at 1.8 GHz and 2.45 GHz frequencies by precisely positioning the slots along with an optimum adjustment of the monopole location and dimensions. The antenna performance increased due to these modifications, which supported its ability to function smoothly at both frequency ranges. The development stages of the antenna are illustrated in Figure 4. The excitation and feeding mechanisms of the monopole were adjusted to improve impedance matching. In addition to introducing a single wing, the length and width of the single wing were modified to enhance the operating range and achieve suitable gains for wireless communication applications. The proposed antenna was designed based on the equations described in [28]:

$$L = \frac{c}{4f\sqrt{\varepsilon_{eff}}} \tag{1}$$

where the operating frequency is f = 1.8 GHz, $c = 3\times10^8$ m/s is the speed of light in free space, L is the length of the monopole antenna, and ε_{eff} is the effective dielectric constant, which is given by:

$$\varepsilon_{\mathrm{eff}} = \frac{\varepsilon_r+1}{2} + \frac{\varepsilon_r-1}{2}\left(\frac{1}{\sqrt{1+12\frac{h}{w}}}\right) \tag{2}$$

where w is the width of the antenna trace, h is the thickness of the substrate, and $\varepsilon_r = 4.3$ is the dielectric constant of FR4.

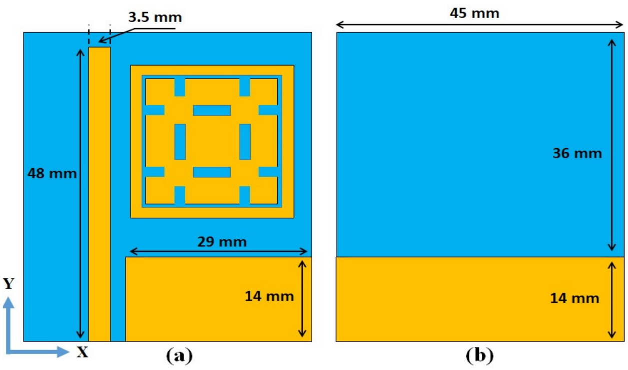

Fig. 3. The geometric configuration of the antenna.

IV. RESEARCH METHODOLOGY

Several published research methods support the creation of miniature antenna designs that use metamaterials together with fractal patterns and meandering lines, and DGS for enabling multiple frequency functionality. Complex technological designs result in both higher production expenses and manufacturing limits that produce multi-dimensional advantages. The slot approach was chosen for the current distribution in dual-band functionality due to its basic structure as well as its simple manufacturing process. This method balances the performance outcomes with design intricacy and sustainable manufacturing capabilities to become applicable to actual world applications.

The methodology to build the dual-band antenna utilizes systematic development steps designed to optimize performance at the target frequencies of 1.8 GHz and 2.4 GHz. The antenna was designed for use in portable devices and ISM band applications; therefore, it should provide consistent and reliable radiation characteristics. Figure 4 demonstrates the various phases of the antenna design method, and Figure 5 shows the return loss for each stage of the proposed antenna design.

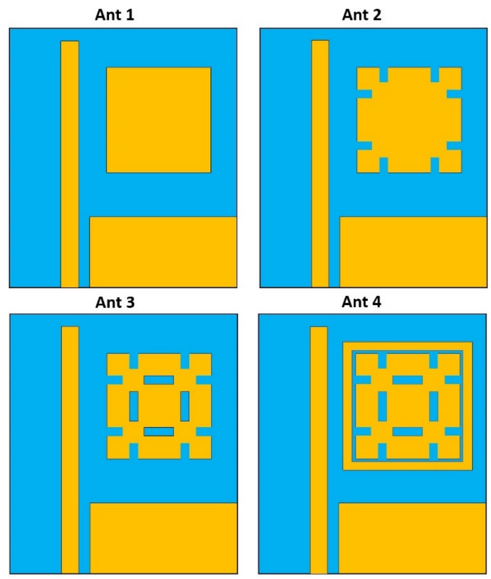

Fig. 4. The stages of the antenna design.

The initially proposed design (Ant 1) consisted of a conventional monopole, a single wing printed on a dielectric substrate at the bottom, a patch element at the upper part, and a partial ground plane on the backside. The second proposed design (Ant 2) is a continuation of the initial design, with rectangular slots cut on the edges of the patch structure. The third design (Ant 3) involved engraving the patch structure with slots. The fourth proposed design (Ant 4) is the final improved version, which involves surrounding the patch structure with a hollow ring. The first design had a reflection coefficient of $|S_{11}|$ <-17 dB at 1.8 GHz, with an operating range of 1.75–1.9 GHz and an emerging band at 2.7 GHz. When the patch structure was deformed with rectangular slots, it was found to have significant effect, as the proposed design resonated at two modes (1.8 and 2.5 GHz). At the center frequency of 1.8 GHz, the antenna had an operating range of 1.68–1.92 GHz and an operating range of 2.4–2.66 GHz at 2.5 GHz. Using the demonstrated patch structure (Ant 3), the proposed antenna was found to resonate in two modes at 1.8 GHz and 2.4 GHz when the slots were inserted into the patch. Nevertheless, matching, return loss, and radiation efficiency need to be improved. The performance of the antenna was enhanced in terms of the reflection coefficient, Voltage Standing Wave Ratio (VSWR), and impedance matching. The performance improvement is attributed to the introduction of the slots in the patch structure, and the introduction of a hollow square ring surrounding the patch to reduce losses and suppress the unwanted surface waves. Introducing slots within the patch structure implies that the distribution and effective electrical properties of the radiator are adjusted to enhance the current distribution and, hence, improve the antenna radiation performance.

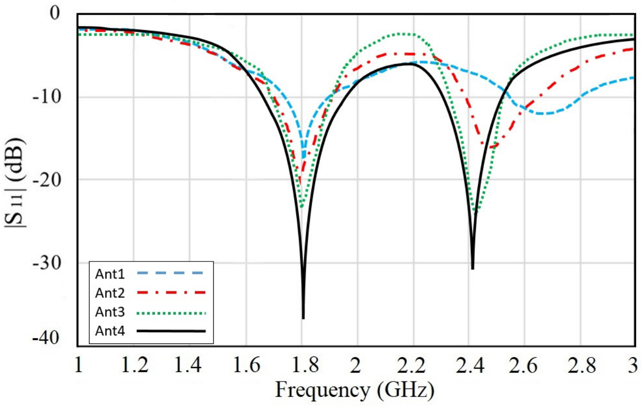

Fig. 5. The return loss for each stage of the proposed antenna design.

The slots disrupt the current flow and create discontinuities while at the same time offering the possibility to increase the electrical length of the antenna without altering the size of the physical antenna. This change also improves the return loss and power transfer from the antenna to the transmission line, as characterized by an improved return loss. Furthermore, the slots remove the undesirable resonant frequencies and cut off the surface wave, which in turn leads to an enhancement in the radiation efficiency and bandwidth. Moreover, the size, shape, and location of the holes employed in the design of the antenna were adjusted to guarantee appropriate matching as well as frequencies appropriate for optimum operation. This technique is useful for providing a relatively straightforward and efficient way to enhance the characteristics of an antenna without major changes in its design.

Figure 6 depicts the effect of varying the wing length on the antenna behavior. The wing dimensions varied from 12 to 16 mm, with a 2 mm increment at each step. It was found that at a wing length of 12 mm, the impedance matching decreased slightly compared to a wing length of 14 mm. This is attributed to the fact that increasing the wing length increases the effective electrical length of the antenna. It was also noted that the operating bandwidth of the proposed antenna is narrower at a wing length of 16 mm at 1.8 GHz. Therefore, in order to achieve the best performance in terms of impedance matching, operating range, and transmission efficiency, the wing length was set at 14 mm.

The implementation of the 1.8 GHz band enhances cellular phone systems that use GSM alongside LTE and specific 5G connections while providing a robust transmission and wide network reach. The 2.45 GHz band serves Bluetooth systems, multiple Wi-Fi (IEEE 802.11), RFID implementations, and industrial control applications, thus enabling a fast data exchange over short operating distances. The proposed antenna design combines 1.8 and 2.45 GHz bands into one platform, providing compatibility with smartphones, IoT devices, and wireless communication systems. The dual-band operation improves the communication reliability and versatility between mobile, industrial, and consumer networks.

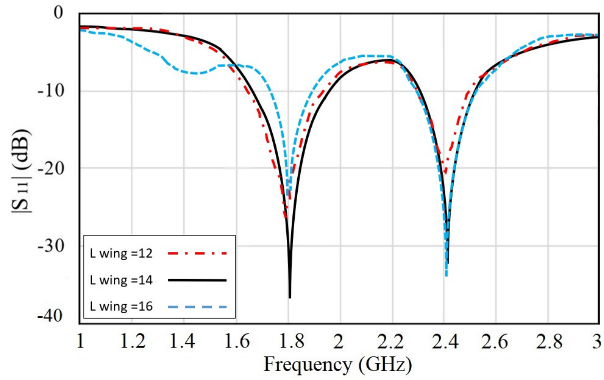

Fig. 6. Effect of changing length wing on antenna performance.

V. RESULTS AND DISCUSSION

The proposed dual-band antenna design achieves resonance matching at two frequencies, as shown in the return loss analysis in Figure 7. The graph displays the |S11| (dB) relative to frequency through two notches, indicating a wide power reflection reduction. The antenna demonstrated efficient radiation while minimizing reflection at its first resonance point of 1.8 GHz and second resonance point of 2.4 GHz with return loss values below -10 dB. The operating bandwidths exist within the shaded regions, proving suitability for dual-band applications. The antenna achieves operating ranges of 1.65–1.97 GHz at center frequency of 1.8 GHz (17.78%) and 2.3–2.52 GHz at center frequency of 2.4 GHz (9.17%), enabling operation at these bands in modern communication systems. The results show that the proposed design functions as expected at the desired frequencies.

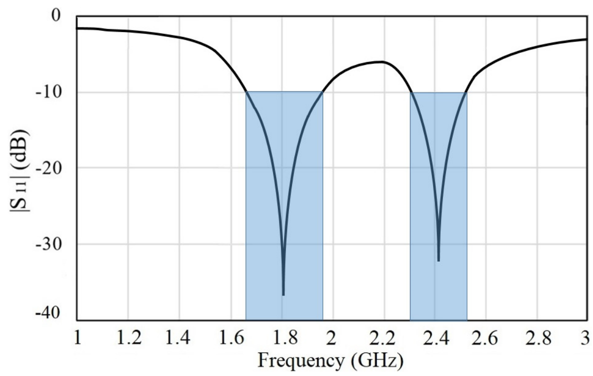

Fig. 7. Return loss analysis of the proposed antenna.

The 3D radiation pattern of the proposed antenna operating at 1.8 GHz is presented in Figure 8a. The antenna achieved the highest gain of 2.045 dBi at 1.8 GHz, which reflects its directional energy concentration abilities. The radiation pattern had an omnidirectional monopole shape, although there were minor changes in gain at different angles. The antenna exhibited a radiation efficiency of -0.3342 dB with a total efficiency of -0.3399 dB, indicating high energy transmission efficiency. The antenna efficiency was calculated using:

$$Antenna\ Efficiency(\eta) = \frac{P_{radiated}}{P_{input}} \quad (3)$$

Alternatively, if the Gain (G) and Directivity (D) of the antenna are known:

$$\eta = \frac{G}{D} \quad (4)$$

In terms of decibels (dB), it can be expressed as:

$$\eta_{dB} = 10 \times log_{10}(\eta) \text{ or } \eta = 10^{\frac{\eta_{dB}}{10}} \quad (5)$$

Therefore, at 1.8 and 2.45 GHz, the antenna achieved radiation efficiencies of 92.59% and 96.75%, respectively. The antenna shows excellent performance at 1.8 GHz, where its stable radiation pattern makes it applicable for GSM, DCS, and various wireless communication applications.

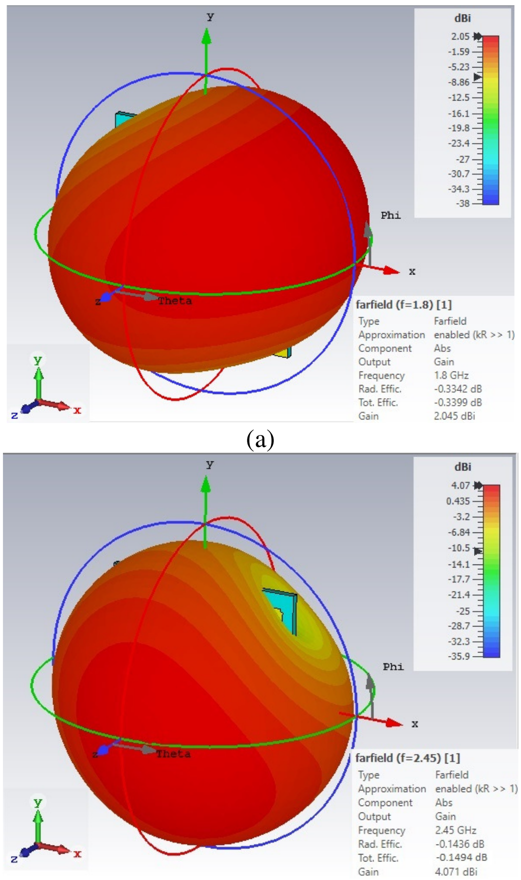

(a)

(b)

Fig. 8. 3D radiation patterns: (a) at 1.8 GHz, (b) at 2.45 GHz.

Furthermore, the 3D radiation pattern of the proposed antenna at 2.45 GHz illustrates omnidirectional radiation capabilities achieving 4.07 dBi max gain according to Figure 8b. The intensity levels appear as a color gradient, with the red areas representing high radiation strength. The antenna performance improves due to the optimized current distribution because the introduced gaps enhance the impedance matching, which results in better radiation performance. The designed modifications enable dual-band functionality without compromising the gain or efficiency, making the antenna appropriate for Wi-Fi and Bluetooth systems and wireless communication networks.

Based on the radiation pattern analysis shown in Figure 9(a), it is observed that the antenna exhibits omnidirectional characteristics at the H-plane. The radiation pattern at the E-plane exhibits stability and smoothness, which is preferred in ISM applications. The 1.8 and 2.45 GHz 2D radiation patterns of the designed slotted antenna appear in Figure 9(b) under E-plane (Phi = 0°) and H-plane (Phi = 90°) conditions. The far-field radiation pattern in the E-plane (Phi = 0°) is shown by the red curve, and the H-plane (Phi = 90°) by the blue curve. The E-plane pattern at 1.8 GHz displays omnidirectional characteristics because the antenna generates uniform radiation. The H-plane pattern of the antenna exhibits a figure-eight shape, which indicates directional characteristics along with nulls located at 90° and 270°. The far-field radiation pattern at 2.45 GHz displays the same form as lower frequencies, yet higher frequency levels make the main lobes more focused, which results in better gain capabilities. The airborne antenna directivity increases with frequency because it strengthens the wireless capability of the Wi-Fi and Bluetooth systems and mobile phone transmissions.

The performance improvements were found to be significant in the proposed antenna, as the effect of the slots on the overall performance was greater. In addition, the slots enhance and provide more resonant frequencies that facilitate dual frequency operation at 1.8 and 2.45 GHz by increasing the electrical length of the patch while keeping the physical length the same. The results demonstrate that this technique improves the impedance matching by redistributing the surface current distribution and the feeding point, which leads to better power coupling and a lower returned power (indicated by the increased return loss). On the other hand, the slots also enhance the radiation pattern, since the radiated power is directed to the desired directions, increasing the directivity and the gain. Additionally, they aid in suppressing the undesired surface waves that are autonomous in the substrate as well as improving those related to the radiation intensity. Additionally, the slots can control the distribution of the prying field to optimize the resonance frequencies and generate design freedom to achieve a better optimization of the desired bands. These factors explain the improved dual-band performance, return loss, directivity, gain, and efficiency.

However, the presence of rectangular slots in the antenna design substantially influences the surface currents in the construction of the proposed antenna. By integrating the slots surrounding the radiating element, it becomes feasible to control the distribution of the surface currents. The slots efficiently attenuate the undesired surface currents, minimize the mutual interference between the antenna elements, and improve the radiation properties by manipulating the propagation of electromagnetic signals. Therefore, the antenna's performance is enhanced, leading to a higher radiation efficiency, enhanced gain, and directivity. Furthermore, the slots can minimize the spread of the surface waves and the influence of the neighboring ambient objects. This leads to an enhanced antenna isolation and system efficiency. Figure 10 shows the surface currents at 1.8 and 2.45 GHz.

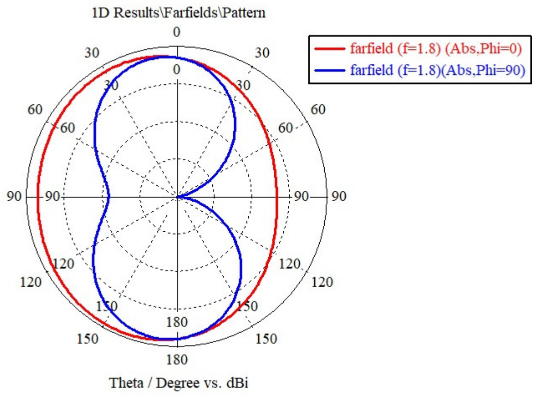

(a)

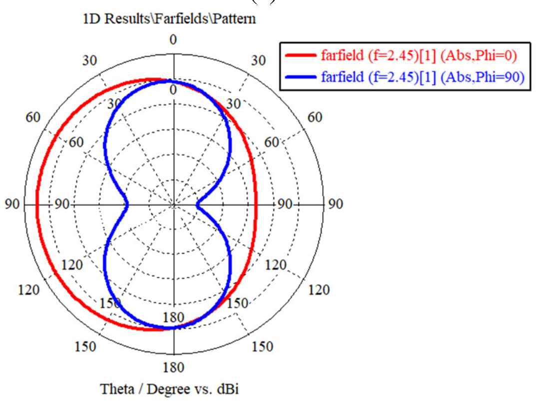

(b)

Fig. 9. 2D radiation pattern analysis: (a) at 1.8GHz and (b) at 2.45 GHz.

An analysis of the surface current density at the various bands used in the operation was conducted to gain a deeper understanding of the functioning of the proposed dual-band antenna. This analysis is illustrated in Figures 10(a) and (b). Figure 10(a) demonstrates that the highest current density is detected together with the stub length at 1.8 GHz. In the case of 2.45 GHz, the flow of the electric current is mostly focused on the single wing and decreases the flow of the current at slots, as shown in Figure 10(b). Upon examining the flux plot at frequencies of 1.8 and 2.45 GHz, it can be seen that the interaction between the slots and the monopole line results in the emergence of two resonance frequencies occurring simultaneously.

The studies listed in Table I demonstrate the performance comparison of the proposed antenna with other studies. In [29], a multi-band antenna for laptop applications was presented. This antenna consisted of a C-shaped strip and an F-shaped strip printed together on an FR-4 substrate. However, the frequency ranges achieved were narrow and the antenna dimensions were large (209 × 260 mm²). Authors in [30] presented a multiband antenna consisting of four S-shaped elements. The antenna system operated effectively in two frequency bands: a broadband covering 1.55–2.65 GHz and a narrower band covering 3.35–3.65 GHz. The antenna was built on an FR4 substrate measuring 58 × 60 mm². However, the size and design complexity limit its use in many applications. In [31], a reconfigurable triangular monopole antenna was proposed for GSM and ISM applications. The antenna was printed on a 40 × 50 mm² ROGERS 5880LZ substrate and achieved an operating range of 1.65–2.51 GHz, with a relatively low gain of approximately 2.2 dB. Authors in [32] presented a low-profile dual-band antenna for wireless sensor applications. The antenna operated at 1.8 and 2.4 GHz bands. The antenna was printed on a 45 × 32 mm² FR4 substrate, and the design parameters were studied to optimize the antenna performance. However, the antenna achieved a weak gain of 1.6 and 1.8 dBi at both frequency bands.

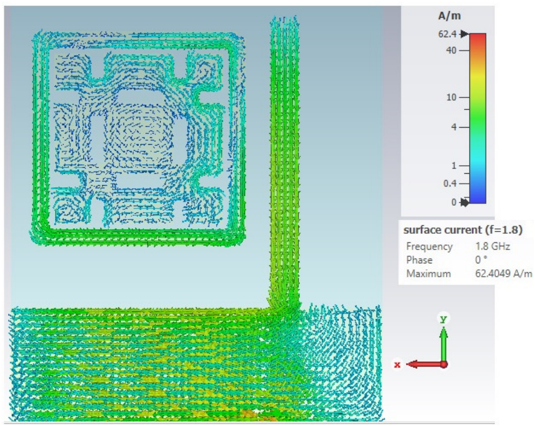

(a)

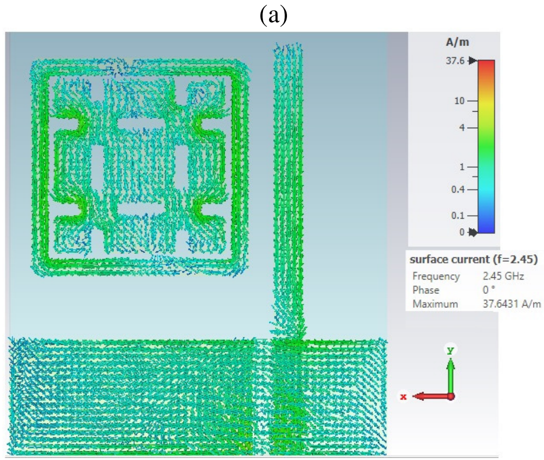

(b)

Fig. 10. Surface currents: (a) surface current concentration at 1.8 GHz, (b) surface current concentration at 2.45 GHz.

The proposed antenna exhibits an enhanced performance relative to that of other antennas, facilitating the dual-band operation, superior impedance matching, and increased gain. In contrast to traditional designs, the integration of slots and ground changes enhances the radiation efficiency while preserving compactness. These enhancements make it more appropriate for wireless applications compared to earlier antennas characterized by a restricted bandwidth or suboptimal efficiency.

TABLE I. EVALUATION OF THE PROPOSED ANTENNA AGAINST CONTEMPORARY TECHNOLOGY

Ref	Sub	Size (mm^2)	Antenna type	Resonance frequencies (GHz)	Gain (dB)
[29]	FR-4	209 × 260	C-shaped	1.8 and 2.4	4.4 and 4.75
[30]	FR-4	58 × 60	S-shaped	1.9 and 3.5	2.2 and 3.8
[31]	ROGERS	40 × 50	triangular	1.75 and 2.25	2.2
[32]	FR-4	45 × 32	PIFA	1.8 and 2.4	1.6 and 1.8
[33]	FR-4	48 × 48	Slotted patch	1.73 and 2.53	-3.8 and 1.9
This work	FR-4	50 × 45	Slotted patch	1.8 and 2.45	2 and 4

VI. CONCLUSIONS

A new slotted monopole antenna was designed and developed to achieve good performance in the two desired frequency bands of 1.8 and 2.4 GHz. The proposed antenna was printed on an FR4 dielectric substrate with an overall size of 50 × 45 × 1.6 mm^3. The incorporation of rectangular slots in the radiating part and partial etching of the ground plane facilitate the impedance matching and optimal performance over the desired bands of operation. The antenna achieved a wide operating range of 1.65–1.97 GHz at a center frequency of 1.8 GHz, representing 17.78%, whereas at a center frequency of 2.4 GHz, the operating range was 2.3–2.52 GHz, representing 9.17%. Compared with modern designs, the proposed dual-band slotted patch antenna exhibits a better trade-off between compactness and performance. With a 50×45 mm² footprint and 2 dB and 4 dB gains at 1.8 and 2.45 GHz, respectively, it exceeds the performance of several other antennas in terms of size, efficiency, and gain. For example, it has greater gain than the PIFA in [32] and the slotted patch in [33] but with similar dual-band operation to larger designs [29].

The main achievement of this study is the development of a miniature dual-band monopole antenna that delivers high performance by using slots and Defected Ground Structures (DGS) strategies. The proposed antenna maintains a flat configuration and one-layer format, which allows standard Printed Circuit Board (PCB) manufacturing. The design blends physical dimensions with impedance range and gain capabilities very well for wireless systems, depending on small antennas with good efficiency levels and excellent impedance matching. As a result, the proposed design offers a new structure and a well-balanced solution that provides a workable substitute for small, dual-band wireless systems.

These results emphasize the novelty and applicability of the proposed design for wireless applications. Future work can focus on reducing the size, incorporating other parts, such as the electromagnetic bandgap, and improving its suitability for other frequencies to enhance its applicability. Finally, this research proves that the use of creative geometric alterations together with pragmatic engineering solutions can yield better antenna performance.

ACKNOWLEDGMENT

The authors are grateful for the support of the Communication Engineering College, University of Technology, Iraq. As a group of lecturers working in this department, they extend their gratitude to the department and their university.

REFERENCES

[1] A. N. Muhi, M. Q. Algburi, H. Abdulkarim, and M. Ghanim, "Innovative Designs for Enhanced Connectivity for 3G and 4G Cellular Networks," in *2024 International Conference on Radar, Antenna, Microwave, Electronics, and Telecommunications (ICRAMET)*, Bandung, Indonesia, Nov. 2024, pp. 56–61, https://doi.org/10.1109/ICRAMET62801.2024.10809318.

[2] C. B. Nsir, J. M. Ribero, C. Boussetta, and A. Gharsallah, "Design of a 1×2 CPW Fractal Antenna Array on Plexiglas Substrate with Defected Ground Plane for Telecommunication Applications," *Engineering, Technology & Applied Science Research*, vol. 11, no. 6, pp. 7897–7903, Dec. 2021, https://doi.org/10.48084/etasr.4558.

[3] Y. E. Hachimi, E. M. Louragli, S. A. N. Arockiam, V. Subramanian, S. Das, and A. Farchi, "Design of a Miniaturized Dual-Band Antenna using Slotted Techniques for 2.45/5.8 GHz Microwave Band RFID Utilizations," *Engineering, Technology & Applied Science Research*, vol. 15, no. 1, pp. 20018–20023, Feb. 2025, https://doi.org/10.48084/etasr.9483.

[4] D. Ghosh, A. Nandi, U. Chakraborty, B. Basu, and S. Choudhury, "Conformal Multiband Antenna for Wearable and Gesture-Sensing Applications," *IEEE Sensors Journal*, vol. 25, no. 1, pp. 670–682, Jan. 2025, https://doi.org/10.1109/JSEN.2024.3493414.

[5] S. Rezaeeahvanouee and Y. Tousi, "Analytical Study of Configurable Multiport Patch Antenna for 2-D Beam Synthesis," *IEEE Antennas and Wireless Propagation Letters*, vol. 24, no. 5, pp. 1109–1113, May 2025, https://doi.org/10.1109/LAWP.2025.3526522.

[6] K. Aafizaa, K. Uma Haimavathi, and S. Saravanan, "Recent Innovations in Microstrip Patch Antennas: Biomedical Uses and Wireless Integration," *Biomedical Materials & Devices*, Feb. 2025, https://doi.org/10.1007/s44174-025-00286-5.

[7] A. A. Abdulhasan, A. J. Salim, and J. K. Ali, "A Swastika-like fractal-based compact quarter-mode substrate integrated waveguide X-Band resonator," *AIP Conference Proceedings*, vol. 3169, no. 1, Feb. 2025, Art. no. 040035, https://doi.org/10.1063/5.0254298.

[8] M. Y. Muhsin, A. J. Salim, and J. K. Ali, "An eight-element multi-band MIMO antenna system for 5G mobile terminals," *AIP Conference Proceedings*, vol. 2651, no. 1, Mar. 2023, Art. no. 060005, https://doi.org/10.1063/5.0105773.

[9] H. Q. Al-Gburi, M. Algburi, and H. Al-Saedi, "Compact Antenna Design for RFID and IoT Applications," in *2022 2nd International Conference on Computing and Machine Intelligence (ICMI)*, Istanbul, Turkey, Jul. 2022, pp. 1–4, https://doi.org/10.1109/ICMI55296.2022.9873727.

[10] B. Yin, P. Chen, L. Tan, X. Fu, and X. Sheng, "Ultra-narrow size slotted sleeve multi-band antenna for mining wireless repeaters," *Electromagnetics*, vol. 45, no. 4, pp. 291–304, May 2025, https://doi.org/10.1080/02726343.2025.2459138.

[11] A. Kumar, M. Aljaidi, M. Singh, M. S. Alshammari, A. A. Alsuwaylimi, and S. M. Alenezi, "Recent Trends in Compact Planar Antennas at 5G Sub-6 GHz and mmWave Frequency Bands for Automotive Wireless Applications: A Review," *Progress In Electromagnetics Research C*, vol. 143, pp. 169–180, 2024, https://doi.org/10.2528/PIERC24022708.

[12] K. Li, T. Dong, and Z. Xia, "Wideband Printed Wide-Slot Antenna with Fork-Shaped Stub," *Electronics*, vol. 8, no. 3, Mar. 2019, Art. no. 347, https://doi.org/10.3390/electronics8030347.

[13] M. A. Gburi and M. Ilyas, "A Novel Design Reconfigurable Antenna Based on the Metamaterial for Wearable Applications," *Journal of*

Physics: Conference Series, vol. 1973, no. 1, Aug. 2021, Art. no. 012042, https://doi.org/10.1088/1742-6596/1973/1/012042.

[14] U. Ali, S. Ullah, A. Basir, B. Kamal, L. Matekovits, and H. Yoo, "Design and SAR Analysis of AMC-Based Fabric Antenna for Body-Centric Communication," *IEEE Access*, vol. 11, pp. 73894–73911, 2023, https://doi.org/10.1109/ACCESS.2023.3295993.

[15] S. M. Ali *et al.*, "Wearable and Flexible Sensor Devices: Recent Advances in Designs, Fabrication Methods, and Applications," *Sensors*, vol. 25, no. 5, Jan. 2025, Art. no. 1377, https://doi.org/10.3390/s25051377.

[16] M. Q. Algburi, *Wearable Antenna Design for Iot and Biomedical Applications*. Saarbrücken, Germany: LAP Lambert Academic Publishing, 2022.

[17] A. L. Sharon Giftsy, U. K. Kommuri, and R. P. Dwivedi, "Flexible and Wearable Antenna for Biomedical Application: Progress and Opportunity," *IEEE Access*, vol. 12, pp. 90016–90040, 2024, https://doi.org/10.1109/ACCESS.2023.3343154.

[18] U. Sharma, G. Srivastava, M. K. Khandelwal, and R. Roges, "Design Challenges and Solutions of Multiband MIMO Antenna for 5G/6G Wireless Applications: A Comprehensive Review," *Progress In Electromagnetics Research B*, vol. 104, pp. 69–89, 2024, https://doi.org/10.2528/PIERB23101904.

[19] M.-A. Chung, K.-X. Chen, C.-C. Hsu, and C.-W. Lin, "A 10 × 10 Multi-Band MIMO Antenna System for LTE, 5G, Wi-Fi 7, and X-Band Communication Applications," *IEEE Access*, vol. 13, pp. 28693–28710, 2025, https://doi.org/10.1109/ACCESS.2025.3540637.

[20] M. Y. Muhsin, Z. S. Muqdad, A. H. Sahar, Z. F. Mohammad, and H. AL-Saedi, "Ultra-wideband Antenna System Design for Future mmWave Applications," *Journal of Telecommunications and Information Technology*, vol. 99, no. 1, pp. 67–73, Mar. 2025, https://doi.org/10.26636/jtit.2025.1.1951.

[21] M. Czyz, J. Olencki, and A. Bekasiewicz, "A compact spline-enhanced monopole antenna for broadband/multi-band and beyond UWB applications," *AEU - International Journal of Electronics and Communications*, vol. 146, Mar. 2022, Art. no. 154111, https://doi.org/10.1016/j.aeue.2022.154111.

[22] S. Saleh, T. Saeidi, N. Timmons, and F. Razzaz, "A comprehensive review of recent methods for compactness and performance enhancement in 5G and 6G wearable antennas," *Alexandria Engineering Journal*, vol. 95, pp. 132–163, May 2024, https://doi.org/10.1016/j.aej.2024.03.097.

[23] A. Ashyap, R. Raad, F. Tubbal, W. A. Khan, and S. Abulgasem, "Comprehensive Review of Wearable Antennas With Flexible Periodic Structures for Body-Effect Mitigation," *IEEE Access*, vol. 13, pp. 22590–22636, Jan. 2025, https://doi.org/10.1109/ACCESS.2025.3536525.

[24] P. Routray and D. Ghosh, "Wide-band metamaterial absorber for sub-6 GHz 5G applications: Reducing specific absorption rate," *AEU - International Journal of Electronics and Communications*, vol. 193, Mar. 2025, Art. no. 155709, https://doi.org/10.1016/j.aeue.2025.155709.

[25] L. C. Paul *et al.*, "A low-profile antenna with parasitic elements and a DGS-based partial ground plane for 5G/WMAN applications," *Discover Applied Sciences*, vol. 6, no. 1, Jan. 2024, Art. no. 22, https://doi.org/10.1007/s42452-024-05669-9.

[26] H. Kisioglu, "Multiband antenna design with a defected ground structure for 5G and X-band applications," *AEU - International Journal of Electronics and Communications*, vol. 190, Feb. 2025, Art. no. 155651, https://doi.org/10.1016/j.aeue.2024.155651.

[27] K. Jaiswal, S. Yadav, N. Yadav, and R. S. Yadav, "Analysis of Different Feeding Techniques of Butterfly-Shaped Patch Antenna with Defected Ground for UWB Application," *IETE Journal of Research*, vol. 68, no. 5, pp. 3647–3656, Sep. 2022, https://doi.org/10.1080/03772063.2020.1773947.

[28] C. A. Balanis, *Antenna Theory: Analysis and Design*, 3st ed. New Jersey: John Wiley & Sons, Inc., 2005.

[29] J. Kulkarni, "Multi-Band Printed Monopole Antenna Conforming Bandwidth Requirement of Gsm/Wlan/Wimax Standards," *Progress In Electromagnetics Research Letters*, vol. 91, pp. 59–66, 2020, https://doi.org/10.2528/PIERL20032104.

[30] W. M. Abdulkawi, W. A. Malik, S. U. Rehman, A. Aziz, A. F. A. Sheta, and M. A. Alkanhal, "Design of a Compact Dual-Band MIMO Antenna System with High-Diversity Gain Performance in Both Frequency Bands," *Micromachines*, vol. 12, no. 4, Apr. 2021, Art. no. 383, https://doi.org/10.3390/mi12040383.

[31] A. Ghaffar *et al.*, "A Flexible and Pattern Reconfigurable Antenna with Small Dimensions and Simple Layout for Wireless Communication Systems Operating over 1.65–2.51 GHz," *Electronics*, vol. 10, no. 5, Jan. 2021, Art. no. 601, https://doi.org/10.3390/electronics10050601.

[32] L. Chen, H. Zhang, Z. Chen, Y. Zhang, J. Yao, and Y. Xing, "Design of Low-profile Dual-band Antenna for IoT Applications," in *2019 3rd International Conference on Electronic Information Technology and Computer Engineering (EITCE)*, Xiamen, China, Oct. 2019, pp. 1805–1809, https://doi.org/10.1109/EITCE47263.2019.9095024.

[33] M. Wang, L. Yang, and Y. Shi, "A dual-port microstrip rectenna for wireless energy harvest at LTE band," *AEU - International Journal of Electronics and Communications*, vol. 126, Nov. 2020, Art. no. 153451, https://doi.org/10.1016/j.aeue.2020.153451.